Available online at www.sciencedirect.com
ScienceDirect
International Journal of Mass Spectrometry 263 (2007) 179–184
International Journal of Mass Spectrometry
www.elsevier.com/locate/ijms

Low energy electron stimulated desorption of ions from whole human blood

Sylwia Ptasińska *, Léon Sanche

Groupe en Sciences des Radiations, Faculté de Médecine, Université de Sherbrooke, Sherbrooke, Québec, Canada J1H 5N4

Received 27 December 2006; received in revised form 24 January 2007; accepted 26 January 2007
Available online 6 February 2007

Abstract

We present the results of experiments on positive and negative ion desorption, from whole dried samples of human blood and red blood cell (RBC), induced by the impact of electrons with energies below 70 eV. Such bombardments induce a rich fragmentation pattern of cations in comparison to that for negative ions. The threshold for desorption of cations is observed around 20 eV, whereas anions can be formed with electron energy as low as 2 eV. The electron energy dependence of ion yields for all detected anions (H^-, CH_3^-/NH^-, O^-/NH_2^- and OH^-) exhibits resonant structures attributed to the dissociative electron attachment process. The similarity between the line shapes of the ion yield functions of O^- desorption from the blood sample and a pure oxygen molecular film suggests that this anion originates from the ($Fe–O_2$) unit in hemoglobin. Additionally, from the observed shift of peaks in the O^- yield, the binding energy of the oxygen molecule to iron is estimated to be approximately 1.2 eV.

Keywords: Dissociation electron attachment; Ion desorption; Ionization

1. Introduction

The investigation of biological systems present at surfaces, ranging from the simplest models such as water, and amino and nucleic acids, to proteins, DNA, phospholipid membranes, to cells and living tissue, is of considerable interest to a broad interdisciplinary area [1]. Basic research using various experimental probes (electrons, photons, ions, AFM tips, etc.) is driven not only by a large number of applications, such as tissue engineering, biosensors, DNA and proteomic chips for drug development, precision/individualization in medical diagnostics and bioelectronics, but also by curiosity and the importance of understanding the "living state".

An increase in attention to the interactions of low energy electrons (LEEs) with condensed matter (i.e., liquids to solids) has arisen, since high-energy particles interacting with a complex molecular network in a living cell generate electrons with energies lower than 70 eV [2–4] as the most abundant secondary species. It is well accepted that the main biological effects are usually not produced by high energy radiation particles, but rather by the action of the secondary species, which are generated along the ionization track in the cell [5]. Therefore, the investigation of the actions induced by these electrons, not only on simple cellular components, but also eventually on more complex arrangements such as blood-forming stem cells is essential to understand the effects of radiation in different tissues.

Blood is a highly specialized tissue consisting of cellular material (such as red blood cells or RBCs (96%), white blood cells (3%), platelets (1%)) and plasma, which is essentially an aqueous solution containing proteins (8%) and trace amounts of other materials [6]. One of the most important functions of blood is the transport of oxygen from the lungs to all tissues within the body. The oxygen molecule is bound to hemoglobin (Hb), which is the major protein of RBC [7]. Measured blood oxygenation shows that about 98.5% of the oxygen in a sample of arterial human blood is chemically combined with Hb. Only 1.5% of O_2 is physically dissolved in the other blood liquids and not connected to hemoglobin. Deoxygenated blood returning to the lungs is still approximately 75% saturated by O_2. Previous studies on the exposure of fresh blood samples to γ-rays showed a remarkable sensitivity to reaction at the (FeO_2)

* Corresponding author. Fax: +1 819 564 5442.
E-mail address: sylwia.ptasinska@usherbrooke.ca (S. Ptasińska).

1387-3806/$ – see front matter © 2007 Elsevier B.V. All rights reserved.
doi:10.1016/j.ijms.2007.01.022

center in Hb molecule [8]. Secondary electrons, generated in any region of the protein by ionization radiation, can migrate within the hemoglobin to give almost exclusively $(FeO_2)^-$ units.

Moreover, mass spectrometry studies on blood samples may be used to diagnose a patient's health status, for forensic identification, and also to estimate the risk of disease [9]. It has been known that the composition of blood is affected by tumors and by treatment with chemotherapy or radiation. Blood is also the major avenue for the metastasis of cancer cells, as well as for the delivery of anticancer agent to tumors. Recently, the mass spectra obtained by laser induced acoustic desorption of human red blood cells from healthy and anemic male adults showed a difference in mass between these two types of dehydrated corpuscles [10]. The ability to distinguish between these two types of red blood cells substantiates the utility of this method for biomedical applications. Particularly, the selectivity and sensitivity of negative ion mass spectrometry has the potential to greatly aid in the detection of cancer. Presently the dissociative electron attachment (DEA) process is widely used to detect explosives [11] and bacteria and bacterial spores which cause food poisoning [12].

In this paper, we report the first results of an investigation on the desorption of ionic fragments from dehydrated solid samples of whole blood induced by electrons with energies in the range 0–70 eV. Additionally, we compare the anion yield functions from whole blood with red blood cell samples, in order to evaluate similarities and/or differences in a complex system and its molecular constituent.

2. Experimental setup

2.1. Sample preparation

Human blood obtained directly from the finger of a 30-year-old female was used for investigation within 24 h without any purification. Red blood cells were separated from the blood by centrifugation at $1500 \times g$ for 20 min at 4 °C. The RBCs were washed with cold 0.9% sodium chloride and centrifuged, the most common method of isolation of red blood cells from the whole blood. Three layers are visible in centrifuged blood; the plasma layer forms at the top (∼55%) and is approximately 92% water. The second layer consists of white blood cells and platelets. The RBCs form the heavy bottom portion of the separated mixture (∼45%) [6].

One microlitre of blood or RBC sample was dissolved with 1 mL of sterile deionized (Millipore) water, and 80 μL of solution was deposited on a chemically-cleaned tantalum surface substrate over an area of 1.3 cm^2 and then frozen at liquid nitrogen temperature. The samples were then lyophilized with a hydrocarbon-free sorption pump at 5 mTorr. After lyophilization, samples were exposed to the atmosphere for approximately 10 min and then were transferred into the ultra-high vacuum load-lock chamber. Tantalum substrates are well known to be fouled by oxidation and contamination by other impurities [13,14]; therefore, relatively thick films (10 ± 1 μm) are usually deposited on them to insure that the measured signal arises from electron interaction with biomolecules.

2.2. Experimental method

A detailed description of the experimental method and the apparatus used in this work are presented elsewhere [15]. Sixteen samples were introduced into a load-lock chamber and were allowed to degas overnight at a pressure of approximately 10^{-8} Torr. Afterwards, the samples were transported into a rotary target holder in the main chamber, via a gate valve, where they were irradiated with low energy electrons. The working background pressure in the analyzing chamber was 5×10^{-10} Torr. An electron beam produced by a custom-made electron gun (ELG-2, Kimball Physics Inc.) was focused on a 2 mm^2 spot. The energy resolution of the beam emitted from a tantalum disc cathode was calculated to be approximately 0.5 eV with an independently adjustable beam current between 1 nA and 10 μA.

It is well known that electron trapping in molecular films depends on the film thickness, i.e., the probability of charge accumulation under LEE impact increases with the film thickness [16]. Due to relatively thick films deposited, the incident electron current was therefore reduced to 5 nA to avoid significant charging of films caused by scattered electrons or ions thermalyzing in the film. Electrons impinged onto the sample in the horizontal plane at an incident angle of 70° to the surface normal. The electron energy scale was calibrated by taking 0 eV as the onset of electron transmission through the film, with an estimated error of about ±0.3 eV [17]. In the present experiments, the sample kept at a fixed position was irradiated by electrons with incident energies of between 0 and 18 eV during 1.7 min. Desorbed negatively and positively ions were analyzed by a quadrupole mass spectrometer (Extrel 150-QC) with its axis positioned perpendicular to the film surface. Mass resolution of this quadrupole ($m/\Delta m$) is 400 in the mass range 1–120 amu.

3. Results and discussion

Below 70 eV, there are three major mechanisms producing ion desorption by electron impact on condensed phase molecules: dipolar dissociation (DD), dissociative ionization (DI), and dissociative electron attachment (DEA). For a diatomic molecule AB these processes may be represented, respectively, by the following reactions:

$$e^- + AB \rightarrow (AB)^* + e^- \rightarrow A^+ + B^- + e^- \quad (1)$$

$$e^- + AB \rightarrow (AB^+)^* + 2e^- \rightarrow A^+ + B + 2e^- \quad (2)$$

$$e^- + AB \rightarrow (AB)^{*-} \rightarrow A + B^- \quad (3)$$

The first reaction proceeds via an excited AB^* state and results in the formation of an ion pair, the second mechanism leads to the formation of positive ions, and the last one involves the formation of a transient negative ion state which dissociates into negatively charged and neutral fragments. In an electron stimulated desorption (ESD) experiment, the DEA is evidence as a peak in the energy dependence of the anion yield [18], since the dissociating transient anion arises from electron capture into an orbital is accessible at a specific energy. In contrast, DD and

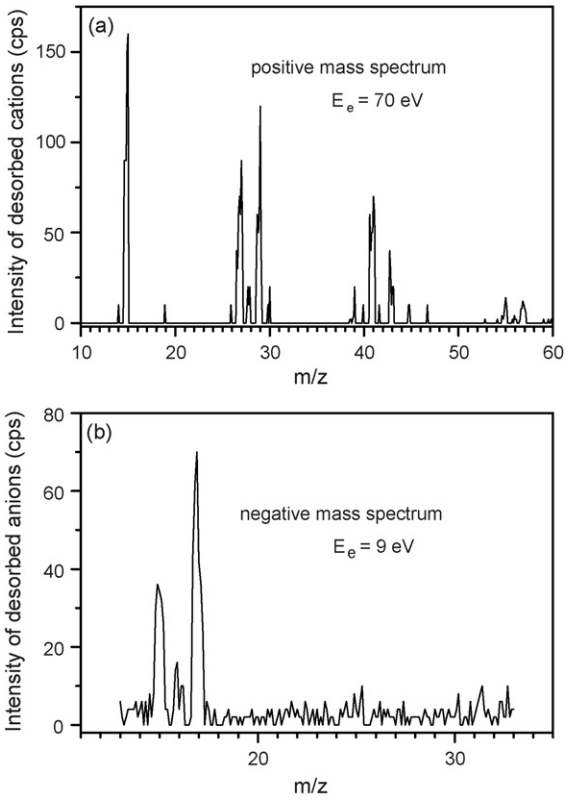

Fig. 1. (a) The positive ion mass spectrum obtained from a whole blood sample at the electron energy of 70 eV. All desorbed cations with possible molecular formula are listed in Table 1. (b) The negative ion mass spectrum recorded at the electron energy of 9 eV.

DI processes involve the transition of the molecules to a dissociative excited state, which is usually produced by non-resonant scattering. The latter interaction is not energy-specific and thus produces a monotonic rise of the fragment signal with increasing electron energy.

Fig. 1 illustrates the positive and negative ion mass spectra of the blood sample in the mass range of 10–60 amu, obtained for electron energies 70 and 9 eV, respectively. Only fragment ions with low molecular weight are detected; the suppression of higher mass fragments is due to two reasons: (1) the process of neutralization, which increases exponentially with the mass of desorbed ion [19] and (2) the decrease in the kinetic energy necessary to overcome the attractive polarization and image charge forces induced by the anion in the molecular film and the metal substrate.

The present mass spectrometric study does not give information about the structure of the ions and the neutral fragments; however, from the mass of the ion and the known atomic composition of the ionic fragment, a molecular formula of the desorbed ion can be obtained. All cations desorbed from whole blood with possible molecular formulas are listed in Table 1.

The present ion mass spectrum of desorbed cations (Fig. 1a) differs from one obtained in ESD of RBCs with the electron beam energy of 2 kV [20]. In the latter case, observed O^+, OH^+, and H_3O^+ were assumed to originate from the water of hydration on the RBC sample. Corresponding ions are detected also in the present work; however, the previous assumption of the formation of these cations based on the presence of H_2O in the blood sample is excluded here and will be explained below. Additionally, in an ESD spectrum reported by Dylla and Abrams [20], fragment ions corresponding to Na^+ and Cl^+ from the saline component of the blood plasma were observed, as well as the peaks at 14 amu which could be assigned as CH_2^+ or N^+. In our work, the dominant desorbed cation in the mass range above 10 amu is a fragment with molecular weight of 15 amu which can be assigned as CH_3^+. Previous secondary ion mass spectroscopy (SIMS) spectrum [20] of the RBC sample taken with 2 kV Xe^+ ions showed many hydrocarbon fragments and also strong saline-related peaks. Moreover, the SIMS spectrum showed more fragmentation than the ESD mass spectra of RBC and whole human blood samples.

The study of desorption spectra, not only gives information about relative yields of ionic fragments, but also provides us with information about threshold energies. In a general picture of ESD, the incident electron occupies one of valence orbitals with antibonding character, which results in the ion desorption due to repulsive potential between atoms. The theoretical threshold for cation desorption is typically low, in the range of 15–20 eV [21,22]. For example, the ion efficiency curves for the most dominant desorbed ion (CH_3^+/NH^+) observed in mass spectrum Fig. 1a and for protonated iron (FeH^+) are shown in Fig. 2. The electron energy onset for producing both ions is measured to be 19 and 20 eV, respectively, with the estimated accuracy of ±0.5 eV (Fig. 2). In the present studies the corresponding threshold is estimated from a value of an electron energy at which the cation signal is discernable. For all observed cations from the studied samples, the estimated values of thresholds are above 20 eV (not shown here). The series of ESD studies for different condensed molecules containing methyl groups indicate that the nature of the predesorption final states gives rise to both H^+ and CH_3^+ desorption [23]. The threshold for CH_3^+ is equal

Table 1
Cations desorbed from whole blood samples with possible chemical formulas

Mass of desorbed cation fragments (amu)	Molecular formula
15	HN^+
	CH_3^+
27	CHN^+
	$C_2H_2^+$
28	CO^+
	CH_2N^+
	$C_2H_4^+$
	N_2^+
29	CHO^+
	CH_3N^+
30	NO^+
	CH_2O^+
	CH_4N^+
41	$C_2H_3N^+$
43	$HCNO^+$
55	–
57	HFe^+

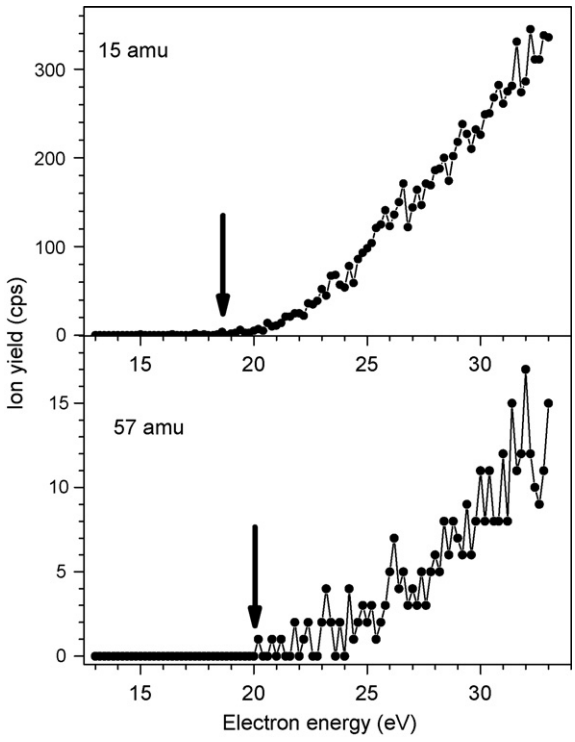

Fig. 2. The ion emission intensity recorded at masses 15 and 57 amu vs. incident electron energy from a blood sample, showing the desorption threshold energy of 19 eV (upper panel) and 20 eV (lower panel), respectively.

for all studied hydrocarbons and for the corresponding cation in the present studies. These results suggest that in organic solids, the highest desorption yield is mainly observed from terminal (functional) groups within molecule [23].

The negative ion mass spectrum (Fig. 1b) recorded at an electron energy of approximately 9 eV is less complex than that for positive ions. The difference is explained by the different nature of the processes for formation of negatively and positively charged ions by low energy electrons [24]. The anion mass spectrum clearly shows three peaks at masses of 15, 16, and 17 amu, which can be identified as CH_3^-/NH^-, O^-/NH_2^- and OH^-, respectively. For all negative ions, several DEA resonances below 18 eV are observed both for a film of whole blood or RBC (see Fig. 3). The positions of maxima in anion yields are listed in Table 2, where the estimated accuracy is on the order of ±0.5 eV. The yields for all observed anion fragments desorbed from RBC resemble quite well those from whole blood in regards to the shape and intensity of ion yields for both samples with the same thickness. The observed similarities in ion yields are expected due to the fact that in the whole blood sample, water (the main compound of plasma) and gases can be removed during lyophilzation and pumping. The ion yield for H^-, the most dominant desorbed anion from both samples, shows a maximum at 9.1 eV (Fig. 3a). Generally, light H^- ions are much less susceptible to post-dissociation neutralization when leaving the surface than heavy ions, which spend a long time close to the substrate surface. Thus, H^- ions exhibit higher yields than, for example, O^- and OH^- ejected from the same organic films, in spite of the respective electron affinities of 0.75, 1.46 and 1.82 eV, which strongly favor the heavy ions.

Table 2
Electron energy of the peaks for all anions desorbed from whole blood sample

Desorbed anion	Electron energy (eV)
H^-	9.1
CH_3^-/NH^-	9.0
O^-/NH_2^-	8.8
	13.0
	15.1
OH^-	6.6
	12.0
	16.4

Moreover, the H^- formation from small organic molecules in the gas phase indicates remarkable site-specificity in DEA depending on functional groups [25–27]. Similarly, site selectivity can be expected for anion desorption as a consequence of the site dependent binding energies of hydrogen atoms in these molecules. The results of D^- ion desorption induced by LEEs incident on condensed deuterocarbons showed that a maximum of ion yields was observed at energy of 9–10 eV [28]. Whereas the yield function for H^- from molecules which posses OH as functional group, e.g., water [29] and methanol [30], exhibits the desorption peak around 7 eV. Thus, the observed maximum in the ion yield of H^- can be attributed to the production of hydrogen anions from the carbon sites of molecules in the blood sample. The origin of H^- at 9.1 eV is also most likely from the methyl group. Hemoglobin, the main component of blood, has

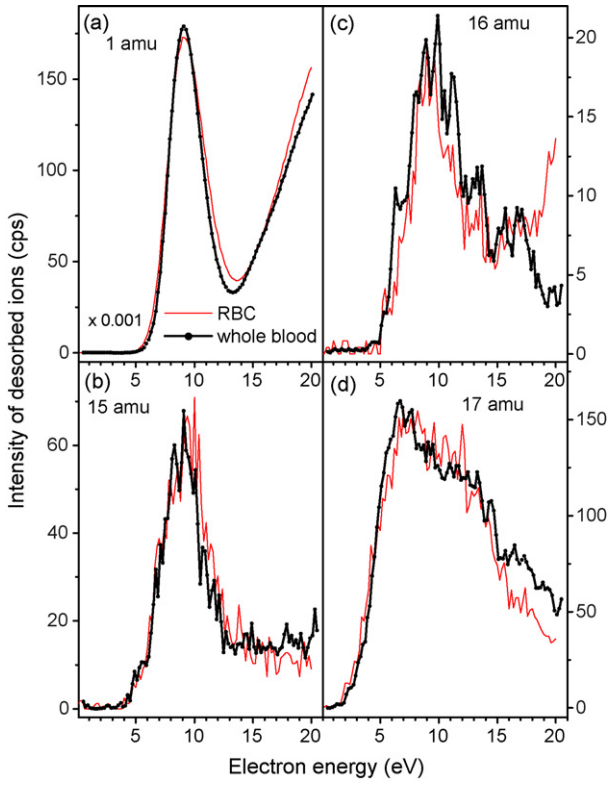

Fig. 3. (a–d) The electron energy dependence of the electron stimulated desorption yields of anions recorded at masses 1, 15, 16 and 17 amu, respectively, from a whole blood sample and red blood cells.

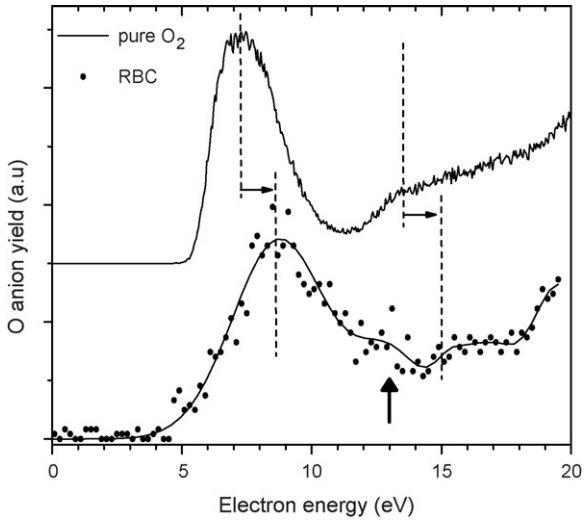

Fig. 4. The O^- ion yields as a function of electron energy obtained from RBC sample and film of pure O_2 film (the data taken from ref. [32]).

four CH_3 groups in its structure. In the present experiment, the ion yield recorded at mass 15 amu exhibits a peak at 9 eV, similar to that for hydrogen anions, with a small shoulder at 5 eV (Fig. 3b). This ion can be attributed to the formation of methyl radical anion (CH_3^-) and/or imidogen anion (NH^-). The resolution of the present mass analyzer does not allow identification of those ions. However, according to recent studies on ESD from the peptide backbone [31], the desorption of anions with mass 15 amu can be ascribed due to dissociation of a core-excited transient anion located on the methyl group.

From a biological point of view, it is very important to investigate the formation of the oxygen anion, which can result from dissociation of O_2 during electron irradiation. The ion yield of O^-, presented as a function of electron energy in Fig. 3c, displays two structures peaking at 8.8 and 15.1 eV. The observed signal for this anion arises most probably from an oxygen molecule bound to iron in the porphyrin ring. The ionizing radiation studies, where the blood samples were exposed to γ-rays, showed that electron capture at the (Fe–O_2) units in hemoglobin is remarkably selective [8]. The extra electron is evenly distributed between iron and dioxygen rather than being extensively delocalized into the porphyrin ring [8].

This O^- yield shape resembles that obtained from pure O_2 films [32], although in the present studies resonant structures are shifted towards higher energies (Fig. 4). The DEA to O_2 in the condensed phase leads to O^- formation peaks near 7.3 and 13.5 eV and the continuous increase of the signal above 17 eV. The latter signal is attributed to the production of O^- via nonresonant DD. The shift of desorption peaks observed around 1.2 and 1.6 (±0.5) eV, respectively, in the present experiment can be due to the O_2 binding to iron in the hemoglobin molecule via the reaction

$$e^- + (\text{Fe–O}_2) \rightarrow (\text{Fe–O}_2)^{*-} \rightarrow \text{Fe} + {O_2}^{*-} \rightarrow \text{Fe} + \text{O} + \text{O}^- \quad (4)$$

From previous studies on the dynamics and equilibrium O_2 binding behaviour in various iron porphyrin systems [33], a standard reaction enthalpy for the oxygen molecule binding to hemoglobin was estimated to lie between −13.6 and −15.5 kcal/mol (0.6 and 0.7 eV). This value is in agreement, within error bars with the shift of the first peak in the O^- yield function recorded in our experiment. Moreover, compared to condensed O_2, an additional structure is observed in the energy dependence of O^- at 13 eV, which can originate from desorption of an oxygen anion from DEA to other compounds of blood.

The second most abundant anion desorbed from blood is the hydroxyl anion (OH^-), presented in Fig. 3d. The OH^- detection is observed over a wide range of electron energies (2–20 eV) and clearly shows two visible maxima at 7 and 12.5 eV. The origin of OH^- is ambiguous owning to the complexity of the protein mixture and the large number of components in blood. However, the possibility of hydroxyl ion desorption from water molecules can be excluded due to the fact that the OH^- yield function does not resemble that observed from pure films of water [34]. Moreover, the ratio of intensities of OH^- yields from water [34] and RBC is much smaller than one [OH^- (water)/OH^- (blood) $\ll 1$] under similar experimental conditions. This suggests that observed signal of hydroxyl anion origins from proteins in blood samples.

4. Conclusion

In this investigation, positively and negatively charged ion desorption induced by low energy electron impact on whole blood and red blood cell samples has been observed. The energy onsets for desorbed cations lie at around 20 eV. In contrast, anions are produced at energies much below this threshold. The yields for all observed anion fragments desorbed from RBC resemble quite well those from whole blood in regards to the shape and intensity of ion yields for both samples. It is known that proteins, either in the membrane or cytoplasmic fraction of RBC are identified through a unique set of peptides and amino acids; a characteristic which is exclusive to a given protein. Nevertheless, analytical methods cannot distinguish between identical peptides originating from different proteins [7], since similar proteins may contain regions of identical sequence. In the present work the interpretation of the origin of ions desorbed by electron bombardment is consistent with that for the peptide backbone [31]. However, the high abundance of Hb in red blood cells limits the detection of low quantities of other proteins, so that the signals for all ions in the present work are mainly attributed to hemoglobin.

Additionally, all of these results have an important bearing on the question of what happens when living tissue is exposed to ionizing radiation. Prior to the present investigations, the action of the LEEs produced in large quantities by ionizing radiation has been studied in the isolated systems consisting of films of a unique biomolecule or a mixture with H_2O [35]. The results reported herein already show that fundamental electron–molecule processes, such as DEA, are still present and equally effective in a much more complex and biological environment such as dried human blood and red blood cells. Furthermore, it would be interesting in future work to investigate the magnitude of ESD of ions from blood samples of patients with leukemia and other blood-related diseases in order to look

into the possibility of developing tools for the early detection of cancer or other diseases.

Acknowledgements

This work is financed by the Canadian Institutes of Health Research (CIHR). The authors would like to thank Mr. P. Cloutier and Mr. Z. Li for technical support. S. Ptasińska would like to thank the CIHR for financial support in the form of a fellowship.

References

[1] B. Kasemo, Surf. Sci. 500 (2002) 656.
[2] International Commission on Radiation Units and Measurements, ICRU Report 31, ICRU, Washington DC, 1979.
[3] J.A. La Verne, S.M. Pimblott, Radiat. Res. 141 (1995) 208.
[4] V. Cobut, Y. Frongillo, J.P. Patau, T. Goulet, M.-J. Fraser, J.-J. Jay-Gerin, Radiat. Phys. Chem. 51 (1998) 229.
[5] C. von Sonntag, The Chemical Basis for Radiation Biology, Taylor and Francis, London, 1987.
[6] D. Shier, R. Lewis, J. Butler, Hole's Human Anatomy & Physiology, 9th Edition, McGrew Hill, 2002.
[7] D.G. Kakhniashvili, L.A. Bulla Jr., S.R. Goodman, Mol. Cell. Proteomics 3 (2004) 501.
[8] M.N.O. Bartlett, J.M. Stephenson, M.C.R. Symons, Proc. R. Soc. Lond. B 238 (1989) 103, and references therein.
[9] J. Roboz, Mass Spectrometry in Cancer research, CRC Press, 2002.
[10] W.-P. Peng, Y.-Ch. Yang, M.-W. Kang, Y.-K. Tzeng, Z. Nie, H.-Ch. Chang, W. Chang, Ch.-H. Chen, Angew. Chem. Int. Ed. 45 (2006) 423.
[11] D.S. Moore, Rev. Sci. Instrum. 75 (2004) 2499.
[12] M.B. Beverly, K.J. Voorhees, Anal. Chem. 72 (2000) 2428.
[13] T. Thundat, L.A. Nagahara, P.I. Oden, S.M. Lindsay, M.A. George, W.S. Glaunsinger, J. Vac. Sci. Technol. A 8 (1990) 3537.
[14] K.S. Rothenberger, B.H. Howard, R.P. Killineyer, A.V. Cugini, R.M. Enick, F. Bustamante, M.V. Ciocco, B.D. Morreale, R.E. Buxbaum, J. Membr. Sci. 218 (2003) 19.
[15] S. Ptasińska, L. Sanche, J. Chem. Phys. 125 (2006) 144713.
[16] M. Michaud, E.M. Hébert, P. Cloutier, L. Sanche, J. Appl. Phys. 100 (2006) 073705.
[17] K. Nagesha, J. Gamache, A.D. Bass, L. Sanche, Rev. Sci. Instrum. 68 (1997) 3883.
[18] L. Sanche, Phys. Rev. Lett. 53 (1984) 1638.
[19] H.D. Hagstrum, Phys. Rev. 119 (1960) 940.
[20] H.F. Dylla, J.H. Abrams, Scan. Electr. Microsc. III (1984) 1219.
[21] D. Menzel, R. Gomer, J. Chem. Phys. 41 (1964) 3311.
[22] P.A. Redhead, Can. J. Phys. 42 (1964) 886.
[23] J.A. Kelber, M.L. Knotek, Phys. Rev. B 30 (1984) 400.
[24] H.S.W. Massey, Negative Ions, Cambridge University Press, London, 1976.
[25] S. Ptasińska, S. Denifl, V. Grill, T.D. Märk, E. Illenberger, P. Scheier, Phys. Rev. Lett. 95 (2005) 093201.
[26] S. Ptasinska, S. Denifl, V. Grill, T.D. Märk, P. Scheier, S. Gohlke, M.A. Huels, E. Illenberger, Angew. Chem. Int. Ed. 44 (2005) 1647.
[27] V.S. Prabhudesai, A.H. Kelkar, D. Nandi, E. Krishnakumar, Phys. Rev. Lett. 95 (2005) 143202.
[28] P. Mozejko, A.D. Bass, L. Parenteau, L. Sanche, J. Chem. Phys. 121 (2004) 10181.
[29] P. Rowentree, L. Parenteau, L. Sanche, J. Chem. Phys. 94 (1991) 8570.
[30] L. Parenteau, J.P. Jay-Gerin, L. Sanche, J. Phys. Chem. 98 (1994) 10277.
[31] P. Cloutier, C. Sicard-Roselli, E. Escher, L. Sanche, J. Phys. Chem. B 111 (2007) 1620.
[32] A.D. Bass, L. Parenteau, M.A. Huels, L. Sanche, J. Chem. Phys. 109 (1998) 8635.
[33] J.P. Collman, J.I. Brauman, B.L. Iverson, J.L. Sessler, R.M. Morris, Q.H. Gibson, J. Am. Chem. Soc. 105 (1983) 3052, and the reference therein.
[34] X. Pan, H. Abdoul-Carime, P. Cloutier, A.D. Bass, L. Sanche, Radiat. Phys. Chem. 72 (2005) 193.
[35] For a review see L. Sanche, Eur. Phys. J. D 35 (2005) 367.